JOURNAL OF PHYSICAL ORGANIC CHEMISTRY, VOL. 8, 452–462 (1995)

INTERMOLECULAR INTERACTIONS THAT DETERMINE THE REGIOSELECTIVITY IN 1,3-DIPOLAR CYCLOADDITIONS OF *N*-METHYL-1,3-OXAZOLIUM-5-OLATES WITH *N*-(PHENYLMETHYLENE)BENZENESULPHONAMIDE

L. BONATI*
Dipartimento di Chimica Fisica ed Elettrochimica, Università degli Studi, Via Golgi 19, 20133 Milan, Italy
R. FERRACCIOLI*
CNR, Centro di Studio sulla Sintesi e Stereochimica di Speciali Sistemi Organici, Via Golgi 19, 20133 Milan, Italy
AND
G. MORO
Dipartimento di Chimica Fisica ed Elettrochimica, Università degli Studi, Via Golgi 19, 20133 Milan, Italy

1,3-Dipolar cycloadditions of *N*-(phenylmethylene)benzenesulphonamide with mesoionic *N*-methyl-1,3-oxazolium-5-olates give 2,5-disubstituted imidazole derivatives with high regioselectivity. The intermolecular interactions underlying this regioselectivity were investigated. The conformational and electronic properties of the reagents were characterized separately. The approach in the early stages of the reactions was then modelled by considering the steric and electrostatic molecular interactions. The interaction energies related to different reaction paths were calculated by perturbation molecular orbital (PMO) treatment and compared.

INTRODUCTION

The reactions between *N*-phenylsulphonylimines and mesoionic *N*-methyl-1,3-oxazolium-5-olates, or münchnones,[1,2] provide the first examples of 1,3-dipolar cycloadditions of münchnones with an acyclic C=N double bond[3] to afford imidazole derivatives. The reactions between *N*-(arylmethylene)-benzenesulphonamides and unsymmetrically substituted münchnones proceed with very high regioselectivity.[1]

In this study, we carefully re-examined the 1,3-dipolar cycloadditions of *N*-(phenylmethylene)benzenesulphonamide (**1**) to the münchnones **2a–c**. As shown in Scheme 1, two different paths, A and B, provide two regioisomeric imidazole derivatives **3** and **4**. The initially formed cycloadducts undergo cycloreversion to carbon dioxide and cyclic azomethine ylides, which, on losing benzenesulphinic acid, lead to the corresponding imidazoles.

Imidazole **3** is the largely preferred regioisomer or even the only one in the reactions of **1** with **2b** and **c** (Table 1). The reactions proceed with high selectivity through the same regiochemical path, independent of the substitution patterns, which are opposite in **2b** and **c**. These results are different from those reported in 1,3-dipolar cycloadditions of **2b** and **c** to ethyl propiolate, where a *ca* 1 : 1 mixture of regioisomeric pyrroles was obtained.[4,5]

The regioselectivity seems to depend on the nature of the substituent attached to the dipolarophiles, as shown by the results reported for benzoylacetylene and phenylacetylene, on reaction with **2b** and **c**.[5]

The unexpected results obtained with imine **1** prompted us to investigate the molecular interactions determining the regioselectivity.

The regiochemical behaviour of these reactions has not been thoroughly studied from a theoretical point of view. Some reports[5–7] interpreted the regioselectivity of 1,3-dipolar cycloadditions of ethylenes or acetylenes with unsymmetrically substituted münchnones in terms of a qualitative frontier molecular orbital (FMO) analysis. Some of them pointed out[4,6] that this approach was not adequate to predict regioselectivity because long-range contributions, such as electrostatic or

* Authors for correspondence.

CCC 0894–3230/95/070452–11

Received 15 April 1994
Revised 27 February 1995

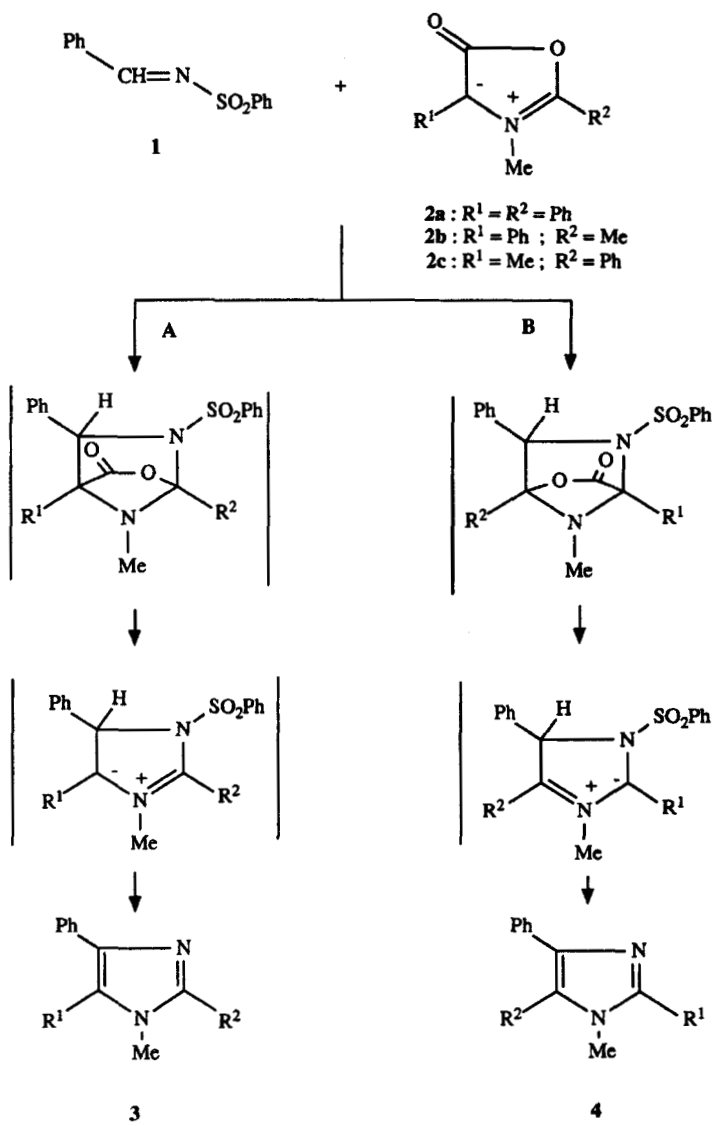

Scheme 1

polarization forces, may be important when compounds with high local charge densities are involved. Therefore, a less approximate perturbation treatment was proposed,[4] taking electrostatic interactions between the reaction centres into account in addition to the developing covalent interactions between the FMOs.

To tackle the problem directly, the full potential energy surface (PES) must be analysed and the transition states (TSs) located and characterized. However, the proper treatment of both the synchronous and non-synchronous paths possibly involved in the cycloaddition reaction mechanism requires computational methods which describe diradicaloid and closed-shell species with the same degree of accuracy.[8-10] In our case molecular dimensions do not allow for calculations of the PES at this computational level; Hartree–Fock TSs, according to recent literature,[11] represent the maximum level achieved for such large systems. Moreover, no assumption can be made concerning the TS geometries or the mechanisms of these reactions, since no test calculations on prototype cycloadditions are available. However, it has been widely demonstrated[12] that a good estimate of the energy sequence in the cycloaddition reaction TS can be

Table 1. Experimental results

Reaction	Yield (%)[a]	Regioisomer ratio[b] 3:4
1 + 2a	64	—[c]
1 + 2b	46	100:0
1 + 2c	49	92:8

[a] Relative to isolated compounds.
[b] The regioisomer ratio was determined by ^{1}H NMR analysis of the crude reaction mixture, within an experimental error of 1%.
[c] Regioisomers are not distinguishable because $R^1 = R^2$.

obtained by assessing the relative stabilities of the adducts formed in the early stages. We therefore decided on PMO treatment of the interaction at these stages as the most suitable approach for rationalizing selectivities in the reactions examined.

A model based on the PMO treatment of Salem and Devaquet,[13] which we previously proposed[12,14,15] for the rationalization of regio-, site- and stereoselectivity of cycloaddition reactions seemed particularly suitable for our purposes. In fact, the structures of the perturbed states, usually fixed arbitrarily at an early point along a hypothetical reaction coordinate, are unbiasedly defined in our model; the van der Waals minima for the alternative reaction paths are assumed as model structures for the corresponding perturbed states. They are located by considering both the non-bonding and the electrostatic contributions to the long-range intermolecular interaction energy.

The method we developed gives a physically meaningful definition of the perturbed state structures even in reactions such as those of **1** with **2a–c**, where bulky reactants are involved and contributions of non-interacting atoms prevail in the long-range interaction. The procedure for locating the perturbed states was carefully re-examined in order to assess this aspect.

COMPUTATIONAL METHODS

Conformational analysis of the two isolated reactants was done with molecular mechanics calculations, using the Tripos force field implemented in the Sybyl program V5.4.[16] The electronic properties of the molecular mechanics minimum energy conformations were calculated with the semi-empirical MNDO method[17] using the MOPAC 5·0 program.[18] To investigate the influence of the computational method on the molecular properties, *ab initio* calculations were also carried out on imine **1** with a 3–21G* basis set, using the Gaussian 90 program.[19]

The weakly interacting complexes formed in the early stages of the reaction, i.e. the perturbed states, were modelled by the corresponding van der Waals minima.[12,14,15] To locate these minima in the intermolecular energy hypersurface, a computer program had already been developed,[20] in which the non-bonded interactions between all the pairs of atoms of the two molecules were described with a Lennard–Jones (6–12) potential function.

The Lennard–Jones parameters for the H, C, N and O atoms were taken from Scott and Scheraga.[21] We calculated parameters for the S atom by the procedure that they adopted (the calculated parameters d_{ij} and e_{ij} in the 6–12 potential[21] for the S···S interaction were $d = 271\,000$ kcal mol^{-1} Å^{12} and $e = 249$ kcal mol^{-1} Å^6; for the mixed interactions, parameters were determined by the combining rules commonly used for this purpose[22]). To improve the description of electrostatic contributions to the interaction energy, an explicit coulombic term was added to the (6–12) function. The resulting potential, usually[22] referred to as (6–12–1), is

$$U_{ij} = d_{ij} r_{ij}^{-12} - e_{ij} r_{ij}^{-6} + Q_i Q_j r_{ij}^{-1}$$

where Q_i and Q_j are the net atomic charges. Mulliken atomic charges determined by the MNDO method were used. Geometric parameters employed as intermolecular variables in searching the minima were reported previously.[12,15]

We previously proposed[15] that whenever contributions of atoms other than the reaction centres prevail in determining the van der Waals minima, the adducts have to be constrained in the region of the non-bonding energy (E_{nb}) hypersurface where the 2pπ orbitals involved in the new bond formation overlap significantly. We developed three constrained procedures to find the most suitable method in searching for the perturbed state. The PMO overlap energy between interacting orbitals must assume negative values during the E_{nb} minimization (C0 procedure); the overlap integrals between the reaction centres must assume only values falling within specific ranges: $S_{CC} \geq 0{\cdot}007$, $S_{CN} \geq 0{\cdot}005$ in the C1 procedure; $S_{CC} \geq 0{\cdot}014$, $S_{CN} \geq 0{\cdot}010$ in the C2 procedure. These ranges were defined on the basis of the corresponding interatomic distances, smaller than 1·1 times and 1·2 times the van der Waals equilibrium distances in the C1 and C2 procedure, respectively. Results with the non-constrained procedure (NC) were compared with those from the constrained procedures.

Finally, the interaction energies for the perturbed states identified in the different reaction paths were obtained within the framework of the second-order perturbation theory by the intermolecular orbital (IMO) treatment of Salem and Devaquet.[13] The interaction energy (E_{int}) expression includes a term (E_{ovr}) which depends on the overlap between the interacting orbitals and a term (E_{pol}) which takes polar effects into account:

$$E_{int} = E_{ovr} + E_{pol}$$

As indicated previously, E_{ovr} is the sum of repulsive and attractive terms [E_{rep} and E_{mix} in equations (2) and

(3) in Reference 14) and E_{pol} is defined as the summation of coulombic interactions between net atomic charges on all the atoms [equation (4) in Rf. 14)].

RESULTS AND DISCUSSION

Conformational analysis

Four minimum energy conformations were obtained for the imine **1**: two more stable *E* conformations with regard to the C=N double bond and two *Z* conformations with energies about 20 kJ mol^{-1} higher. Both *E* conformations are characterized by the planarity of the Ph–C=N–S moiety and by tetrahedral angles around the sulphur atom. This latter conformational characteristic prevents the phenylsulphonyl group from participating in the π system, which thus involves only the benzylideneimine residue. The spatial disposition of the phenyl ring bonded to the sulphur atom distinguishes the two *E* conformations. In one of these, the C_4 atom lies in the same plane as the Ph–C=N–S moiety and the C(7)–C(4)–S(3)–N(2) torsional angle is 43° (see Figure 1 for the atom numbering). A preliminary analysis of the interaction between the münchnone **2a** and **1**, taken in this conformation, showed that steric hindrance due to the rotated phenyl ring inhibits their approach: in the resulting van der Waals minima the intermolecular distance was 4·5–5·0 Å.

In the light of these results, in the subsequent analysis we considered the other *E* conformation of **1**, in which the phenyl ring and an oxygen atom point out of the plane with torsional angles C(4)–S(3)–N(2)–C(1) and O(5)–S(3)–N(2)–C(1) of 60·5° and −54·2°, respectively. The electronic properties were calculated for this conformation.

Mulliken population analysis by the MNDO method indicated (Table 2) a strong polarization of the C=N double bond towards the nitrogen atom and a high positive charge on the sulphur atom, balanced by negative charges on all the atoms bonded to it. This behaviour was confirmed by a single-point calculation performed *ab initio* with a 3–21G* basis set (Table 2).

On the basis of the geometry optimization on **2a–c**, a unique conformational minimum for each molecule was achieved. This minimum was characterized by a planar five-membered ring with phenyl substituents twisted about 40–45° with respect to it, as indicated by x-ray data.[23] The partial rotation does not inhibit $p\pi$ orbital overlap and allows the phenyl rings to participate in π conjugation with the five-membered ring.

Among the resonance structures proposed for münchnones,[24,25] the double-bond character we obtained

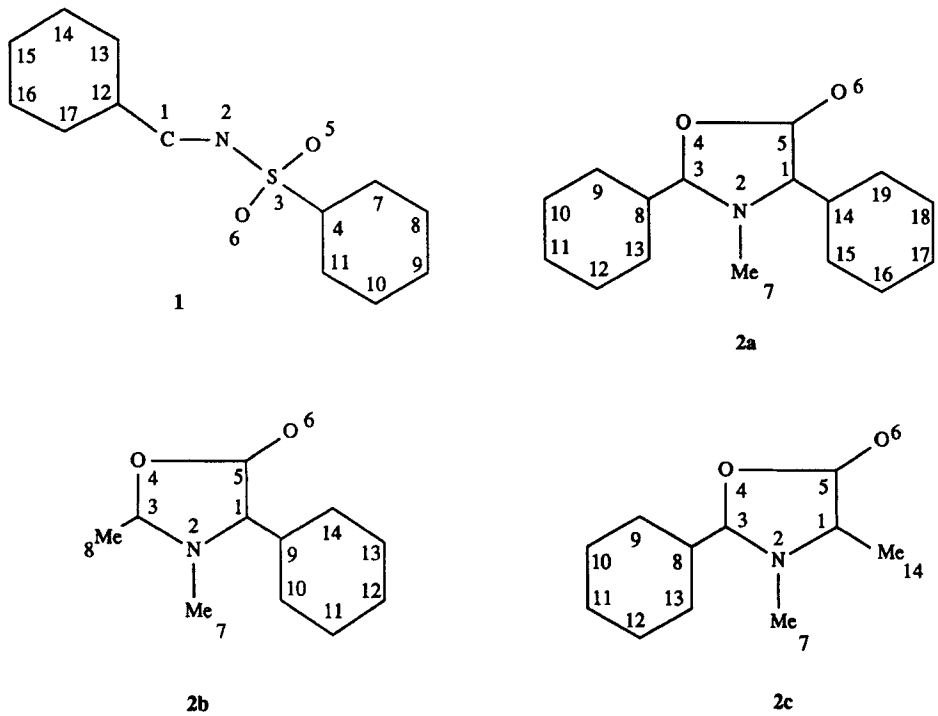

Figure 1. System for atom numbering

Table 2. *N*-(Phenylmethylene)benzenesulphonamide (**1**): atomic Mulliken charges with hydrogens summed into heavy atoms

Atom[a]	MNDO	3–21G[a]
C(1)	0·327	0·512
N(2)	−0·580	−0·749
S(3)	1·798	1·668
C(4)	−0·502	−0·501
O(5)	−0·750	−0·612
O(6)	−0·694	−0·575
C(7)	0·121	0·073
C(8)	−0·005	0·017
C(9)	0·064	0·033
C(10)	−0·005	0·017
C(11)	0·148	0·083
C(12)	−0·130	−0·177
C(13)	0·057	0·043
C(14)	−0·007	0·012
C(15)	0·049	0·034
C(16)	−0·007	0·013
C(17)	0·117	0·109

[a] See Figure 1 for the atom numbering.

for the C–N bonds and the exocyclic C–O bond, and also the values of the π orbital charges (Q_π in Table 3), indicate that the mesoionic system of **2a–c** is well represented by the formula shown in Scheme 1.

The Mulliken total atomic charges (Q in Table 3) indicate that the most electron-rich centres are C(1), N(2), O(4) and O(6) and the most positive are C(5), C(3) and the methyl groups (see Figure 1 for the atom numbering).

Perturbed states

To rationalize the regioselectivity of the reported reactions through PMO analysis, we needed to define all the possible interaction pathways leading to the different stereo- and regio-adducts. The imine can approach either the upper face of the münchnone, leading to four adducts, denoted Up, or the lower face giving four Down adducts (see Figure 2 for the münchnone orientations). For both approaches, the A and B adducts reflect the two different regiochemical pathways which lead to the **3** and **4** regioisomers (see Scheme 1). The *endo* and *exo* adducts indicate the stereochemistry of the reaction with respect to the reciprocal position of the oxygen atoms in the two molecules. The predictions of facial and stereoselectivity are not experimentally verifiable as the primary cyclo-adducts evolve toward aromatic compounds.

A preliminary analysis of the eight hypothetical adducts for each reaction showed that the electrostatic interaction term is definitely superior to the overlap contribution in determining the interaction energy and that E_{int} is very attractive for the *exo* adducts and very repulsive for the *endo* adducts. We concluded that in the early stages of the interaction the electrostatic forces guide the molecules towards an *exo* approach,

Table 3. Münchnones: atomic Mulliken charges with hydrogens summed into heavy atoms (Q) and π orbital charges (Q_π)

	2a		**2b**		**2c**	
Atom[a]	Q	Q_π	Q	Q_π	Q	Q_π
C(1)	−0·248	−0·384	−0·245	−0·377	−0·315	−0·385
N(2)	−0·153	0·587	−0·142	0·601	−0·129	0·610
C(3)	0·100	−0·121	0·004	−0·149	0·058	−0·152
O(4)	−0·209	0·203	−0·203	0·190	−0·202	0·175
C(5)	0·405	0·192	0·402	0·195	0·400	0·200
O(6)	−0·368	−0·447	−0·365	−0·436	−0·368	−0·432
C(7)	0·303	0·060	0·305	0·061	0·304	0·059
C(8)	−0·035	0·000	0·167	0·054	−0·027	−0·002
C(9)	0·072	0·057	0·036	0·033	0·072	0·053
C(10)	0·008	0·031	−0·021	0·035	0·007	0·027
C(11)	0·027	0·055	−0·000	0·028	0·023	0·049
C(12)	0·007	0·030	−0·000	0·038	0·006	0·026
C(13)	0·016	0·044	0·006	0·032	0·008	0·042
C(14)	0·041	0·030	0·057	0·045	0·162	0·103
C(15)	−0·024	0·023				
C(16)	0·000	0·026				
C(17)	−0·030	0·032				
C(18)	0·007	0·030				
C(19)	0·052	0·044				

[a] See Figure 1 for the atom numbering.

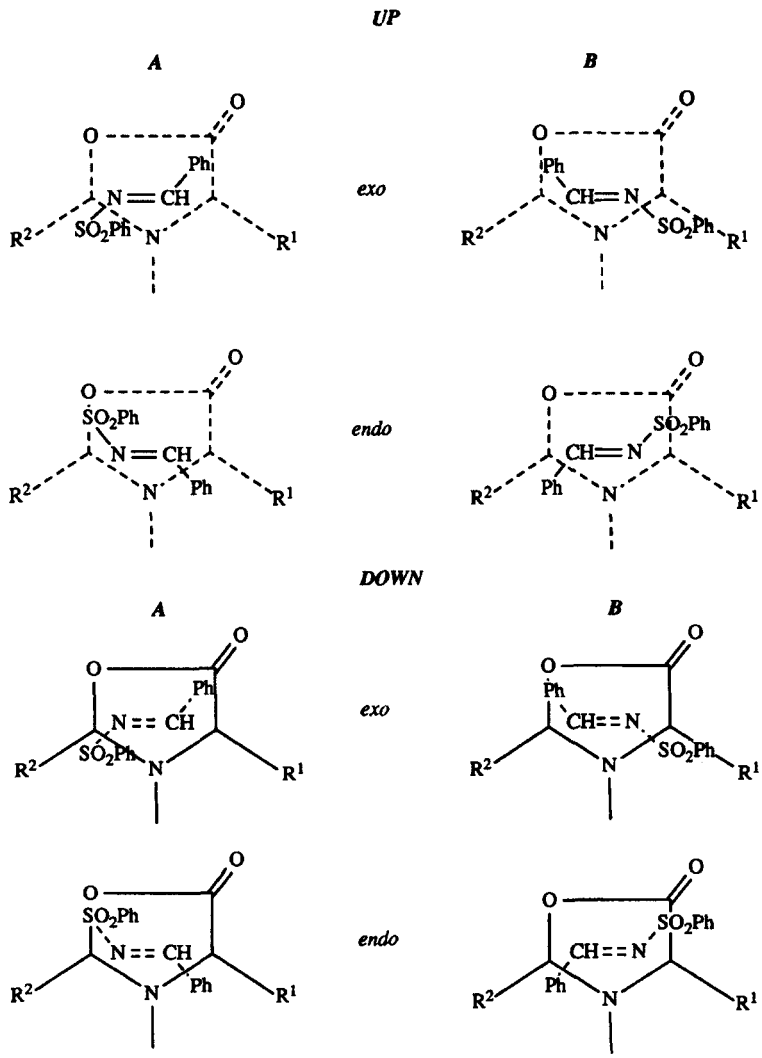

Figure 2. Interaction pathways leading to the different adducts

and omitted the *endo* adducts in the subsequent analysis.

According to our model, we were interested in finding the van der Waals minima in the intermolecular energy surface for the adducts of each reaction. To illustrate the developments in the method proposed to minimize the non-bonding energy we refer to the results for the 'model' reaction of **2a** with **1**, summarized in Table 4 and Figure 3.

For the Down A adduct [Figure 3(a)] the non-constrained minimum geometry is determined not so much by the interactions between atoms directly involved in the new bond formation as by the steric and electrostatic repulsions between their substituents. In particular, the münchnone phenyl rings seem to avoid both the phenyl group and the oxygen atoms of the imine because of steric hindrance. This leads the C=N bond and the münchnone C(1)—C(3) axes to assume cross-shaped arrangement in which the interacting $2p\pi$ orbitals overlap to a lesser extent than in the parallel orientation. In this spatial disposition, similar to all the adducts in the NC minima, the overlap energy is almost null or even repulsive (Table 4).

Hence, to have proper models for the perturbed states, the adducts must be constrained in the region of the non-bonding hypersurface where the $2p\pi$ orbitals on the reaction centres overlap significantly. The minimum geometries obtained by the C0 minimization procedure

Table 4. Energy contributions in the non-bonding energy minima obtained with different minimization procedures[a] for the *exo* adducts of the reaction **1** + **2a**

Adduct	Minimization procedure	D (Å)	E_{pol} (kJ mol^{-1})	E_{ovr} (kJ mol^{-1})	E_{int} (kJ mol^{-1})	E_{nb} (kJ mol^{-1})
Up A	NC	3·71	−12·27	−0·09	−12·36	−56·18
	C0	3·71	−12·27	−0·09	−12·36	−56·18
	C1	3·71	−12·27	−0·09	−12·36	−56·18
	C2	3·53	−13·57	−0·19	−13·75	−50·88
Up B	NC	3·63	−2·31	0·06	−2·24	−57·31
	C0	3·75	−3·99	−0·01	−4·00	−54·42
	C1	3·66	−6·77	−0·05	−6·83	−57·61
	C2	3·49	−3·84	−0·07	−3·91	−40·31
Down A	NC	3·85	−19·48	0·08	−19·40	−66·29
	C0	3·94	−16·31	−0·00	−16·31	−64·40
	C1	3·82	−18·61	−0·05	−18·66	−30·41
	C2	3·50	−21·24	−0·21	−21·45	>100
Down B	NC	3·95	−17·08	0·03	−17·05	−63·86
	C0	4·08	−15·13	−0·00	−15·13	−60·23
	C1	3·83	−14·27	−0·05	−14·32	−32·15
	C2	3·51	−13·47	−0·15	−13·62	19·27

[a] See Computational Methods section.

more clearly describe the molecules' approach in the early stages of the reaction. Although the imine C=N bond remains shifted toward the methyl group, the C=N and C(1)–C(3) axes become virtually parallel and C(3) and N come closer [Figure 3(b)]. Accordingly, the E_{ovr} values in Table 4 become more attractive.

The C0 minima indicate that these bulky reactants lead to perturbed states where the reaction centres are far apart. As a consequence, the overlap energy has little influence on the interaction energy which is almost entirely determined by the electrostatic term.

To verify whether this result depended on the method used to seek the van der Waals minima, the more restrictive minimization procedures C1 and C2 were tested. Figure 3 and the E_{ovr} values in Table 4 indicate that these minima are characterized by more incipient bond formation between the reaction centres than in the C0 minima. Whereas the E_{nb} values in the C0 minima are almost unaffected in relation to the non-constrained values, they increase with the constraint and, for the Down adducts obtained by the C2 procedure, E_{nb} is actually positive. This means that, at the distances imposed in the C1 or C2 procedures, geometrical deformations of the reactants occur. As they cannot be included in the model without going against the PMO theory assumptions, the minima obtained are not satisfactory models for the weakly interacting complexes in the early stages of the reaction.

Therefore, the discussion below of the regio- and stereoselectivities of all the reactions examined refers to the E_{nb} minima obtained by constraining the reactants in the intermolecular region with attractive overlap energy (C0 procedure).

PMO analysis

Energy contributions in the E_{nb} minima, already reported in Table 4 for reaction **1** + **2a**, are shown in Table 5 for the reactions **1** + **2b** and **1** + **2c**. In all the minima the electrostatic term plays a decisive role. The polar interactions between the substituents and those between the reaction centres contribute to this term to a similar extent.

In the reaction of **1** with the symmetrically substituted münchnone **2a**, the electrostatic interactions definitely lead toward a Down facial selectivity. Although there is no marked discrimination between the A and B regioadducts, the first is more stable.

This preference can be explained on the basis of electrostatic interactions between the two reagents in the minimum geometries depicted for the most stable A and B regioadducts in Figure 4(a). In the A adduct interaction between the charged zones of the interacting partners is more favourable. On the one hand, the imine electron-rich nitrogen and oxygen atoms interact with the münchnone electron-poor environment generated by the C(3), the methyl group and the aromatic hydrogens pointing at the sulphonyl group. On the other, the imine C(1) approaches the negatively charged region of the mesoionic system. The low regioselectivity can be related to the long intermolecular distance ($D \approx 4$ Å for both the Down adducts) to which the reagents are confined by the phenyl steric hindrance.

In the reaction **1** + **2c** the minimum geometries are similar to those for **1** + **2a** [compare Figure 4(a) with 4(c)]. The slight increase in A selectivity (see E_{int} values in Table 5) can be explained on the basis of two

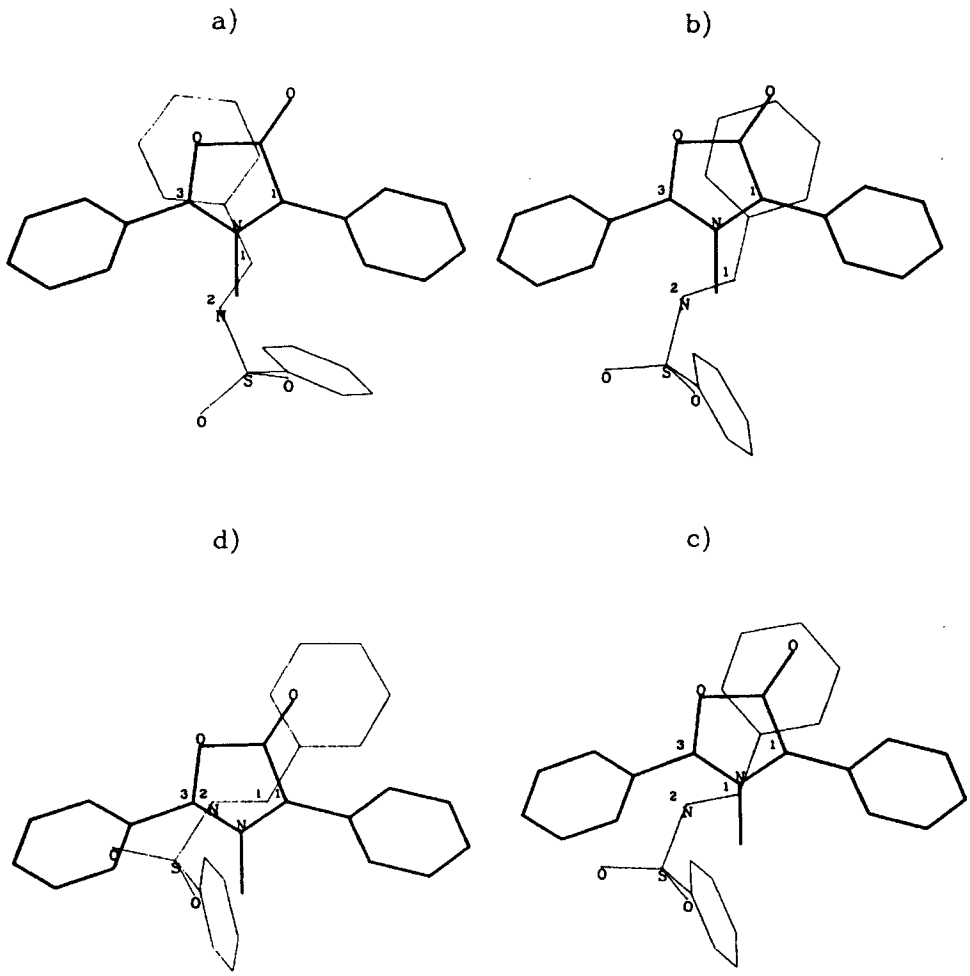

Figure 3. E_{nb} minimum geometries for the Down A *exo* adduct of the reaction **1** + **2a**, obtained with different minimization procedures: (a) Non-constrained, NC; (b) constrained C0; (c) constrained C1; (d) constrained C2

Table 5. Energy contributions in the non-bonding energy minima obtained with the C0 minimization procedure[a] for the *exo* adducts of the reaction **1** + **2b** and **1** + **2c**

Reaction	Adduct	D (Å)	E_{pol} (kJ mol^{-1})	E_{ovr} (kJ mol^{-1})	E_{int} (kJ mol^{-1})	E_{nb} (kJ mol^{-1})
1 + **2b**	Up A	3·65	−16·95	−0·15	−17·10	−55·85
	Up B	3·61	−1·91	−0·00	−1·91	−50·43
	Down A	3·39	−18·72	−0·14	−18·86	−68·77
	Down B	3·99	−12·11	−0·00	−12·11	−54·69
1 + **2c**	Up A	3·61	−4·86	−0·03	−4·89	−65·84
	Up B	3·75	−12·14	−0·01	−12·15	−61·48
	Down A	3·89	−15·36	−0·00	−15·36	−59·67
	Down B	3·60	−10·40	−0·08	−10·48	−58·40

[a] See Computational Methods section.

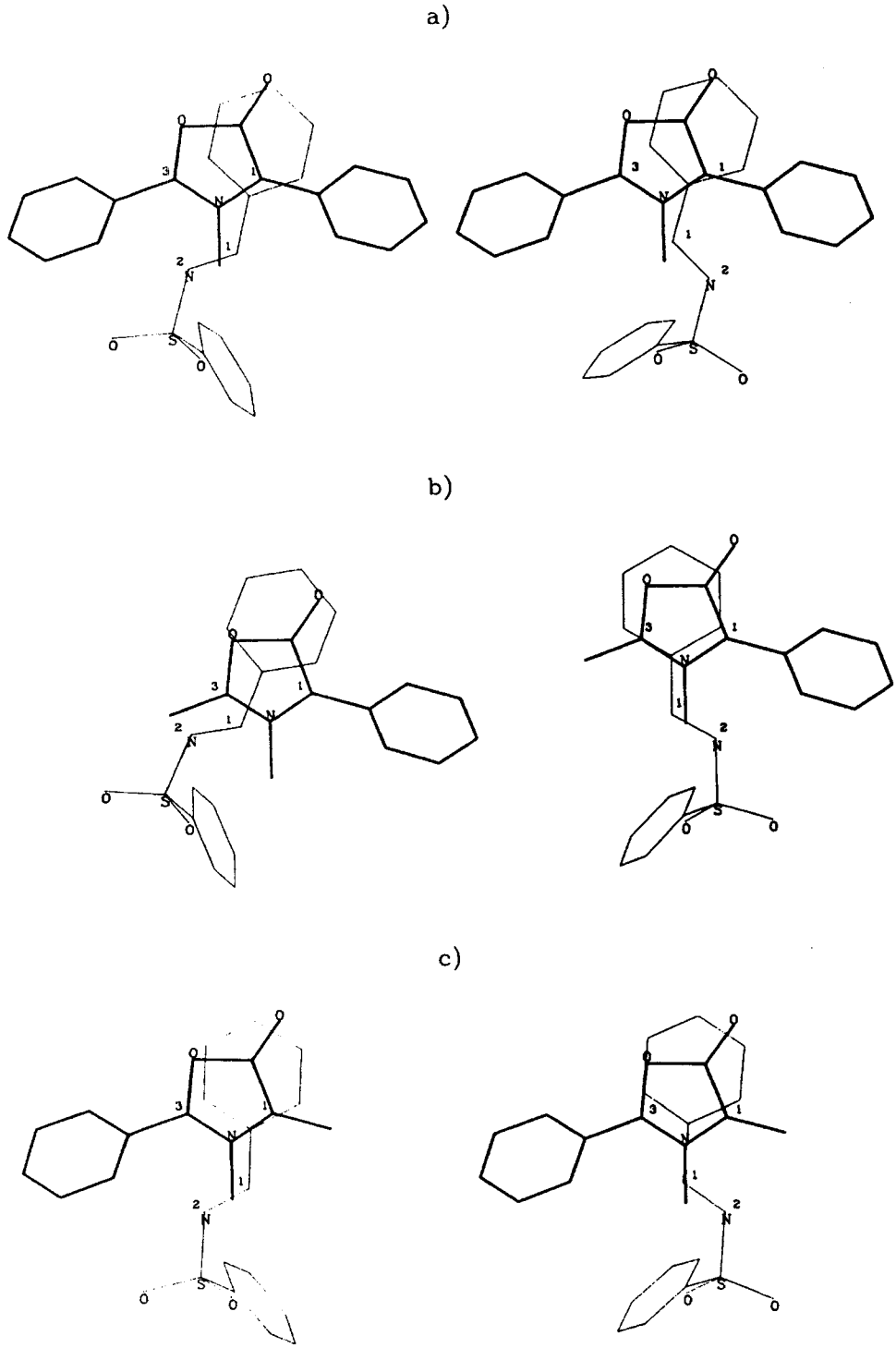

Figure 4. E_{nb} minimum geometries obtained with the C0 minimization procedure for the most stable A and B adducts of the reactions: (a) **1** + **2a**, (b) **1** + **2b** and (c) **1** + **2c**. Left side, A adducts; right side, B adducts

observations. First, a less hindered approach leads to shorter distances between the molecules in the E_{nb} minima (see the D values in Table 5). Moreover, the münchnone C(1) centre, which is made electron richer by the methyl group bonded to it, gives a stronger electrostatic interaction with the positive imine C(1) counterpart in the A adduct.

Inspection of the E_{int} sequence in Table 5 shows that in the **1** + **2b** reaction the A adducts, both Down and Up, are strongly favoured with respect to the B adducts. As shown in Figure 4(b), there is a striking difference in the most stable A adduct geometry in comparison with all the other A minima. The less hindered approach to the münchnone C(3) position explains the shorter intermolecular distance (Table 5) and a disposition of the imine negative centres which makes for more significant electrostatic matching with the münchnone positive environment.

On the basis of these theoretical results, it can be inferred that the reactions examined will mostly follow a regiochemical path A leading to the regioisomer **3**. The reaction **1** + **2a** does not lend itself to any experimental check because of the symmetrically substituted münchnone used, but for the others the experimental results are well verified (Table 1).

An increase of the regioselectivity can be expected on going from the reactions **1** + **2a** and **1** + **2c** to **1** + **2b**. This agrees with the experimentally obtained regioisomer ratio (Table 1).

CONCLUSIONS

Theoretical study of the 1,3-dipolar cycloadditions of **1** with **2a–c** leads to a satisfying rationalization of the high regioselectivity obtained experimentally.

This result further confirms the validity of our PMO model in rationalizing selectivities in cycloaddition reactions. On this basis, we can infer that the electrostatic, in addition to steric factors, must be considered to define the adduct geometries in the early stages of the reaction, particularly when reactants with high local charge densities are involved. Moreover, when lateral substituents make a significant contribution to the long-range interactions, the perturbed state geometries must be obtained by constraining the reactants in the intermolecular region where there is attractive orbital overlap energy. This procedure provides models for the perturbed states which fulfil the PMO theory assumptions.

The energy analysis of the perturbed states obtained shows that electrostatic interactions between the whole molecular charge distributions guide the reagents toward the imidazole derivatives **3**. In the first stage of the A pathway, the interacting molecules assume mutual orientations with higher electrostatic complementarity than in the B path. Reaction **1** + **2b**, where the electrostatic matching is enhanced by the most favourable A adduct geometry, shows the highest regioselectivity.

On the basis of these considerations and previous results,[26] we can infer that the phenylsulphonyl group plays a decisive role in affecting regioselectivity before it is eliminated. It causes strong polarization of the C=N double bond and helps to create a well defined negatively charged portion in the imine molecule. Consequently, the best electrostatic matching is achieved when the imine negative pole is balanced by the münchnone positive counterpart, which remains substantially unaltered in **2b** and **2c** apart from the nature of the C(1) and C(3) substituents.

EXPERIMENTAL

Melting points were measured on a Büchi apparatus and are uncorrected. ^{1}H NMR spectra were recorded on a Bruker AC 300 spectrometer; all chemical shifts are given in ppm from tetramethylsilane as the reference. Positive-ion fast atom bombardment (FAB) mass spectra spectra were determined on a VG Analytical 7070 EQ mass spectrometer with an attached VG Analytical 11/250 data system. Compounds **1**,[27] *N*-methyl-*N*-benzoylphenylglycine,[28] *N*-methyl-*N*-benzoylalanine[28] and *N*-methyl-*N*-acetylphenylglycine[29] were prepared following the methods reported in literature.

General procedure for the reaction of **1** *with* **2a–c**.[1] A solution of dicyclohexylcarbodiimide (2·6 g, 12·6 mmol) in toluene (20 cm^3) was added to a suspension of **1** (8·1 mmol) and the appropriate *N*-acyl-α-amino acid (10·6 mmol) in toluene (40 cm^3). The reaction mixture was stirred at room temperature under a nitrogen atmosphere for 12 h until the starting materials had totally disappeared. The suspension was filtered and the solvent was evaporated at reduced pressure. The residue was taken up in CH_2Cl_2 (50 cm^3) and the solution was washed with 10% $NaHCO_3$ (2 × 30 cm^3) and water. The organic phase was dried (Na_2SO_4) and the solvent removed under vacuum. The mixture was separated by silica gel chromatography using toluene–ethyl acetate (7 : 3) as eluent. In addition to the isolated imidazoles, these reactions gave tar and complex mixtures of side-products which were impossible to separate and identify.

Compound **5** was also isolated from the reaction between **1** and **2b**: yield 6%, m.p. 102–104 °C (from diisopropyl ether). Found C 70·65, H 5·5, N 7·2; $C_{23}H_{22}N_2O_2S$ requires C 70·75, H 5·7, N 7·2; ^{1}H NMR, δ_H (90 MHz; $CDCl_3$) 2·3 (3H, s, 2-Me), 3·3 (3H, s, N-Me), 6·9 (1H, s, CH=), 7·05–7·55 (13H, m, aromatic), 7·85–8·05 (2H, m, aromatic); FAB mass spectrum, m/z 391 (M^+); electron impact mass spectrum, m/z 249 ($M^+ - C_6H_6O_2S$), 208 ($M^+ - C_8H_8NO_2S$). The formation of **5** can be

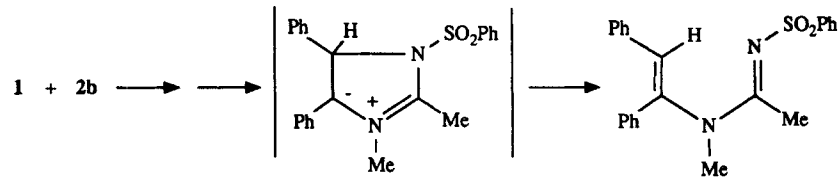

5

Scheme 2

explained by rearrangement of the cyclic azomethine ylide intermediate according to a path involving breaking of the C—N bond,[30] as indicated in Scheme 2.

ACKNOWLEDGMENTS

We thank Emanuela Palma-Modoni for her help with the illustrations. Financial support from the Italian CNR is gratefully acknowledged (Grant No. CT92.00516.CT03 and Progetto Finalizzato Chimica Fine II).

REFERENCES

1. R. Consonni, P. Dalla Croce, R. Ferraccioli and C. La Rosa, *J. Chem. Res. (S)* 188 (1991).
2. P. Dalla Croce, R. Ferraccioli, C. La Rosa and T. Pilati, *J. Chem. Soc., Perkin Trans. 2* 1511 (1993).
3. E. Funke and R. Huisgen, *Chem. Ber.* **104**, 3222 (1971).
4. A. Padua, E. M. Burges, H. L. Gingrich and D. M. Roush, *J. Org. Chem.* **47**, 786 (1982).
5. P. Dalla Croce and C. La Rosa, *Heterocycles* **27**, 2825 (1988).
6. A. Padwa, R. Lim, J. G. MacDonald, H. L. Gingrich and S. M. Keller, *J. Org. Chem.* **50**, 3816 (1985).
7. T. Okano, T. Uekawa, N. Morishima and S. Eguchi, *J. Org. Chem.* **56**, 5259 (1991).
8. F. Bernardi, A. Bottoni, M. J. Field, M. F. Guest, I. H. Hillier, M. A. Robb and A. Venturini, *J. Am. Chem. Soc.* **110**, 3050 (1988).
9. J. J. W. McDouall, M. A. Robb, U. Niazi, F. Bernardi and H. B. Schlegel, *J. Am. Chem. Soc.* **109**, 4642 (1987).
10. Y. Li and K. N. Houk, *J. Am. Chem. Soc.* **115**, 7478 (1993).
11. A. Rastelli, M. Bagatti, A. Ori, R. Gandolfi and M. Burdisso, *J. Chem. Soc., Faraday Trans.* **89**, 29 (1993), and references cited therein.
12. L. Bonati, C. Gatti, G. Moro and D. Pitea, *J. Mol. Struct. (THEOCHEM)* **208**, 235 (1990), and references cited therein.
13. (a) L. Salem, *J. Am. Chem. Soc.* **90**, 543 (1968); (b) L. Salem, *J. Am. Chem. Soc.* **90**, 553 (1968); (c) G. Klopman and R. F. Hudson, *Theor. Chim. Acta* **8**, 165 (1967); (d) A. Devaquet and L. Salem, *J. Am. Chem. Soc.* **91**, 3793 (1969); (e) A. Devaquet, *Mol. Phys.* **18**, 233 (1970).
14. D. Pitea, M. Gastaldi, F. Orsini, F. Pelizzoni, A. Mugnoli and F. Abbondanti, *J. Org. Chem.* **50**, 1853 (1985).
15. L. Bonati, T. Benincori, G. Zecchi and D. Pitea, *J. Chem. Soc., Perkin Trans. 2* 1243 (1991).
16. *Sybyl V5.4*. Tripos Associates, St Louis, MO (1991).
17. M. J. S. Dewar and W. Thiel, *J. Am. Chem. Soc.* **99**, 4899 (1977).
18. K. M. Merz and B. H. Besler, *QCPE Bull.* **10**, 15 (1990).
19. M. J. Frisch, M. Head-Gordon, G. W. Trucks, J. B. Foresman, H. B. Schlegel, K. Raghavachari, M. A. Robb, J. S. Binkley, C. Gonzalez, D. J. Defrees, D. J. Fox, R. A. Whiteside, R. Seeger, C. F. Melius, J. Baker, R. L. Martin, L. R. Kahn, J. J. P. Stewart, S. Topiol, J. A. Pople, *Gaussian 90*. Gaussian Inc., Pittsburgh, PA (1990).
20. G. Moro, L. Bonati and D. Pitea, unpublished work.
21. (a) R. A. Scott and H. A. Scheraga, *J. Chem. Phys.* **42**, 2209 (1965); (b) R. A. Scott and H. A. Scheraga, *J. Chem. Phys.* **45**, 2091 (1966).
22. A. J. Pertsin and A. I. Kitaigorodsky, *The Atom–Atom Potential Method*. Springer, Berlin (1987).
23. G. V. Boyd, C. G. Davies, G. D. Donaldson, G. Silver and P. Wright, *J. Chem. Soc., Perkin Trans. 2*, 1280 (1975).
24. K. T. Potts, in *1,3-Dipolar Cycloaddition Chemistry*, edited by A. Padwa, Vol. 2. Chapt. 8. Wiley, New York (1984).
25. H. L. Gingrich and J. S. Baum, in *Oxazoles*, edited by I. J. Turchi, Chapt. 4. Wiley, New York (1984).
26. P. Dalla Croce, P. Gariboldi and C. La Rosa, *J. Heterocycl. Chem.* **24**, 1793 (1987).
27. *Org. Synth.* 203 (1987).
28. R. Huisgen, H. Gotthardt, H. O. Bayer and F. C. Schaefer, *Chem. Ber.* **103**, 2611 (1970).
29. W. Cocker, *J. Chem. Soc.* 1693 (1937).
30. R. Huisgen, E. Funke, H. Gotthardt and H. L. Panke, *Chem. Ber.* **104**, 1532 (1971).